

Convolutional Neural Networks Quantization with Attention

Binyi Wu

*Faculty of Electrical and Computer Engineering, Technische Universität Dresden, Helmholtzstr. 18,
Dresden, 01069, Germany
binyi.wu@tu-dresden.de, binyi.wu@infineon.com
www.tu-dresden.de*

Bernd Waschneck

*Division of Power and Sensor Systems, Infineon Technologies AG, Königsbrücker Str. 180,
Dresden, 01099, Germany
bernd.waschneck@infineon.com
www.infineon.com*

Christian Georg Mayr

*Centre for Tactile Internet with Human-in-the-loop (CeTI), Technische Universität Dresden, Helmholtzstr. 18,
Dresden, 01069, Germany
christian.mayr@tu-dresden.de
www.tu-dresden.de*

It has been proven that, compared to using 32-bit floating-point numbers in the training phase, Deep Convolutional Neural Networks (DCNNs) can operate with low precision during inference, thereby saving memory space and power consumption. However, quantizing networks is always accompanied by an accuracy decrease. Here, we propose a method, double-stage Squeeze-and-Threshold (double-stage ST). It uses the attention mechanism to quantize networks and achieve state-of-art results. Using our method, the 3-bit model can achieve accuracy that exceeds the accuracy of the full-precision baseline model. The proposed double-stage ST activation quantization is easy to apply: inserting it before the convolution.

Keywords: Quantization; attention; convolutional neural networks.

1. Introduction

To enable neural networks to function on edge devices, researchers have developed various optimization methods in the past few years, such as quantization¹, pruning^{2,3}, and neural architecture search⁴. These methods optimize the network from different perspectives and are not mutually exclusive. Our work mainly studies network quantization.

Quantization not only saves storage costs by several or even tens of times, but it also reduces computing complexity by switching from floating-point to integer operations. Both optimizations brought by

quantization are especially beneficial for embedded devices that run neural networks with limited memory and computing resources. Most of the current deep learning libraries, such as TensorFlow⁵ and PyTorch⁶, only support mature 16/8-bit quantization without loss of accuracy. However, for applications targeting extremely low costs, 16/8-bit quantization is still insufficient.

Previous work^{7–9} has shown that networks inference with low bit-width is feasible, and milestone progress has been made. On the other side, given the great success of the attention mechanism on CNNs,

we found that it also helps to quantize the networks. Based on the previous work, ST quantization¹⁰, we further study the application of the attention mechanism in network quantization. We upgrade ST to double-stage ST, which is illustrated in Section 3. Section 4 demonstrates the experimental results. The conclusion part completes the paper. The proposed double-stage ST quantization overcomes the hardware-unfriendly-input-channel-wise quantization in ST and further improves the accuracy of low-precision networks. In particular, the accuracy of the 3-bit model exceeds the accuracy of the baseline model.

2. Related Work

For network optimization, there are quantization, pruning, and neural architecture search. Quantization optimizes the network at the lowest level, that is, the basic operation unit (the multiplication and accumulation operation). Pruning improves efficiency by cutting very weak or useless filters at the kernel level. NAS searches for the best network at the architectural level and combines different blocks to form an efficient network.

The quantization of the network starts with the quantization of weights. Ref. 11 uses three values of weights +1, 0, and -1 to infer the network. It proves the feasibility of weight quantization. However, the performance benefit is restricted when only the weights are quantized. Because the operation is still floating-point-based and the runtime memory used to store activations remains unchanged. To further improve inference performance, activation also needs to be quantized. However, activation quantization is more problematic due to the usage of non-differentiable operators, which causes the gradient backpropagation to be erroneous.¹² The commonly used solution is to approximate the quantization operation to a straight-through estimator (STE)¹³. In binarization, Ref. 12 is the first to propose method of training Binary Neural Networks (BNNs). In the forward path, the sign function is employed for binarization, while in the backward path, STE is used. Binarization replaces arithmetic operations with bitwise operations, XOR, which boosts efficiency significantly. However, it comes at the high expense of accuracy. Ref. 14 proposes a new binarization function, SignSwish, as well as a regularization term to improve the convergence and generalization ac-

curacy of binary networks. Researchers discovered that the limited representational capability of binary causes the decay. Therefore, subsequent research focuses on enhancing the binary network representation. Firstly, Ref. 15 created the scaling factors to scale the activation, which improves the top-1 accuracy by more than 16% when compared to the previous state-of-the-art works. However, the introduced scaling factors have the same size as the activation and are of full precision. Therefore, in the later work Ref. 16, the scaling factors were reduced to be spatially and channel-wise. Unlike previous works of Refs. 15, 16, Ref. 17 chooses to strengthen the feature expression by connecting real activations to binary activations via a skip connection. In the end, it significantly strengthens the network expression ability, and the top-1 accuracy of the binary network was again greatly improved by 5%. The previous work is mainly based on the existing network architecture, but they are not necessarily suitable for BNN. So afterward, researchers have successively studied the network architecture specific to BNN. With a dedicated BNN architecture, BinaryDenseNet¹⁸ achieved another milestone and significantly exceeded all other 1-bit CNNs by more than 6%. In addition, Ref. 19 demonstrated an architecture composed of DenseBlock and ImprovementBlock and proved such a network can improve feature capacity and feature quality. Whereas Ref. 9 observes that the performance of the binary network is sensitive to changes in the activation distribution. Therefore, they developed RSign and RReLU from Sign and ReLU to explicitly learn distribution variations with almost no added cost. Because the binarization operation will cause the information loss in the activation forward and gradient backward, the performance gap between the full-precision model and the binary model is established. To overcome this problem, Ref. 20 developed an information retention network, IR-Net, to maintain information in the forward activation and backward gradient.

For multi-bit quantization, Ref. 21 introduced DoReFa-Net to train multi-bit neural networks using gradients in non-full-precision. However, the ReLU non-linearity approximation in quantization causes the gradient mismatch. To address this, Ref. 22 offered a half-wave Gaussian quantizer (HWGQ) that approximates the quantizer using activation statistics. However, the multi-bit networks still suffer from

accuracy degradation. To bridge the gap, Ref. 7 developed parameterized clipping activation (PACT), which has a parameter for learning the activation clipping value and is optimized by back-propagation. It is the first time that a 4-bit network can achieve accuracy comparable to full precision networks across a variety of popular models and datasets because to the power of gradient. Whereas Ref. 23 recommends using a full-precision auxiliary module to train the low-precision network, which updates the parameters with additional full-precision routes. To address the non-differentiable problem of quantization, Ref. 24 proposed a differentiable quantization approach, which is done by turning continuous weights and activation distributions into categorical distributions using the quantization grid. Afterward, with these continuous agents, the quantization is done with gradient-based. Different from Ref. 24 but similar to PACT, LSQ⁸ introduces learnable parameters in the quantizer. But the new parameter is for learning step size instead of clipping value. Eventually, they made the 3-bit models reach the full precision baseline accuracy. Like LSQ, Ref. 10 is also for learning quantization interval, but it utilized the power of the attention mechanism and it is realized with the squeeze and threshold (ST) block. Recently, Ref. 25 presented differentiable dynamic quantization (DDQ), a fully differentiable technique to learning bitwidth, clipping value, and quantization interval.

3. Our Approach

Squeeze-and-threshold (ST) block was proposed in Ref. 10 to learn the activation quantization threshold. It utilizes the information of activations itself to quantize the activations. Moreover, the real-value ST branch bypasses the quantization step and can fully back-propagate the gradient to the previous layers. However, the activation quantization in ST is input channel-wise and output channel-wise. It is not consistent with the TensorFlow-Lite⁵ or PyTorch⁶ quantization, in which the activation quantization is only output channel-wise. The difference makes the network inference not so efficient on currently available hardware. Therefore, in this work, we propose an improved version. Its final activation quantization is only output channel-wise. Furthermore, we extend the ST block to be double stages and further improve the performance of the quantized networks. In

the following content of this section, we will detail the improved method, the double-stage ST. For ease of illustration, we adapt the following notations: The tensor in the expression is in bold. Notation H , W and C represent the height, width, and channel, respectively, while N could be the batch of activation or number of filters. Lastly, notation \mathbb{B} is the bit width.

3.1. Activation Quantization

The integration of double-stage-ST-based activation quantization into a network is shown in Fig. 1. The activation quantization corresponds to the part marked with green and blue color, named **ActiQuan**. With our quantization solution, the network architecture stays the same as before quantization.

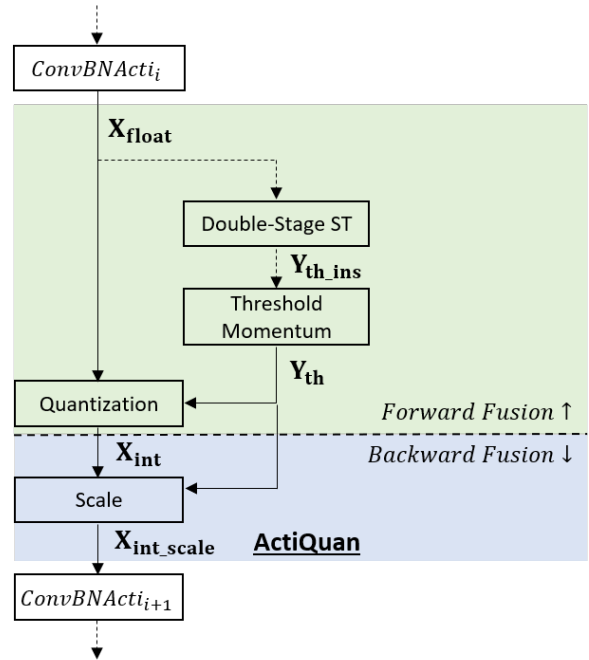


Figure 1. Integration of double-stage-ST-based activation quantization, **ActiQuan**, into networks. \mathbf{X}_{float} is the full-precision activation from previous layer with a shape of $[N, H, W, C]$. \mathbf{Y}_{th_ins} is the instant activation quantization threshold with a shape of $[1, 1, 1, C]$. \mathbf{Y}_{th} has the same shape as \mathbf{Y}_{th_ins} and is iteratively updated by \mathbf{Y}_{th_ins} . \mathbf{X}_{int} is the integer activation having $2^{\mathbb{B}}$ kinds of values. \mathbf{X}_{int_scale} is the full-precision activation but with only $2^{\mathbb{B}}$ options.

The double-stage-ST block extracts the instant threshold \mathbf{Y}_{th_ins} from each batch input activations.

Then $\mathbf{Y}_{\text{th-ins}}$ iteratively updates the final threshold \mathbf{Y}_{th} with

$$\mathbf{Y}_{\text{th}}^+ = (1 - \mathbb{M}) \times \mathbf{Y}_{\text{th}}^- + \mathbb{M} \times \mathbf{Y}_{\text{th-ins}},$$

where \mathbf{Y}_{th}^+ and \mathbf{Y}_{th}^- are the newly updated and previous threshold, respectively. \mathbb{M} is the threshold update coefficient and changes along with training,

$$\mathbb{M} = \mathbb{M}_{\min} \times \left(1 - \cos\left(\frac{\mathbb{E}_{\text{cur}}}{\mathbb{E}_{\text{tol}}}\right)\right) + \cos\left(\frac{\mathbb{E}_{\text{cur}}}{\mathbb{E}_{\text{tol}}}\right),$$

where \mathbb{M}_{\min} is a hyperparameter, the minimum momentum factor. \mathbb{E}_{cur} and \mathbb{E}_{tol} are the current training epoch and total training epochs, respectively.

In quantization, each channel of activation is quantized with the corresponding threshold in \mathbf{Y}_{th} ,

$$\mathbf{X}_{\text{int}} = \begin{cases} \text{sign}(\mathbf{X}_{\text{float}}) * 0.5 + 0.5, & \text{if } \mathbb{B} = 1 \\ \text{clip}(\text{round}(\frac{\mathbf{X}_{\text{float}}}{\mathbf{Y}_{\text{th}}}, \mathbb{V}^-, \mathbb{V}^+), & \text{if } \mathbb{B} > 1 \end{cases}$$

where $\text{sign}(\cdot)$ and $\text{round}(\cdot)$ are the signum and rounding functions, respectively. For multi-bit quantization, \mathbf{X}_{int} is clipped in the range of $[\mathbb{V}^-, \mathbb{V}^+]$ by the clipping function $\text{clip}(\cdot)$. For pure positive activation, $\mathbb{V}^- = 0$ and $\mathbb{V}^+ = 2^{\mathbb{B}} - 1$, otherwise, $\mathbb{V}^- = -2^{\mathbb{B}-1}$ and $\mathbb{V}^+ = 2^{\mathbb{B}-1} - 1$. In the backward path, the non-differentiable functions $y = \text{sign}(x)$ and $y = \text{round}(x)$ are approximated by $y = \text{sigmoid}(4x)$ and $y = x$, respectively.

To maintain the activation statistics and still limit its value with only $2^{\mathbb{B}}$ possibilities.

$$\mathbf{X}_{\text{int-scale}} = \text{mean}(\mathbf{Y}_{\text{th}}) \times \mathbf{X}_{\text{int}},$$

where $\text{mean}(\cdot)$ obtains the mean value of the input tensor. With this setting, the final quantization is compatible with the quantization flow in TensorFlow and PyTorch and is also friendly for currently available hardware.

3.2. Double-Stage Squeeze-and-Threshold

Fig. 2 shows the construction of the double-stage squeeze-and-threshold (ST) block, which is for learning instant activation quantization threshold.

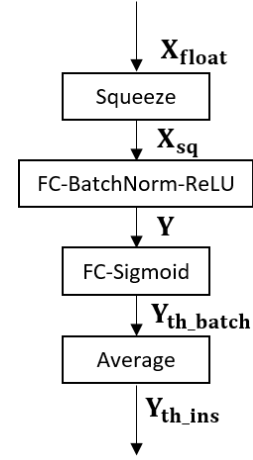


Figure 2. Double-Stage squeeze-and-Threshold block.

The squeeze operation is done with a global average operation, generating $\mathbf{X}_{\text{sq}} \in \mathbb{R}^{N \times 1 \times 1 \times C}$. Compared with ST^{10} , an additional fully-connected-batch-normalization-ReLU layer (denoted as FC-BatchNorm-ReLU in Fig. 2) is added to increase the non-linearity, producing $\mathbf{Y} \in \mathbb{R}^{N \times 1 \times 1 \times C}$. Subsequently, \mathbf{Y} is transferred to activation quantization threshold $\mathbf{X}_{\text{th_batch}} \in \mathbb{R}^{N \times 1 \times 1 \times C}$ by a fully-connected-sigmoid layer. The final average operation computes the arithmetic mean over $\mathbf{X}_{\text{th_batch}}$ along the batch axis, generating the channel-wise activation threshold, $\mathbf{Y}_{\text{th-ins}} \in \mathbb{R}^{1 \times 1 \times 1 \times C}$.

3.3. Inference Optimization

The data only flows through the double-stage ST branch in the training phase. In the inference phase, the iteratively updated \mathbf{Y}_{th} will be used instead. Therefore, double-stage ST block will not introduce computation overhead during inference. In this section, we illustrate how to reconstruct the parameters and operations of **ActiQuan**.

In TensorFlow-Lite⁵, the quantized convolution-batch-normalization-relu layer will be optimized into

$$\begin{aligned} \mathbf{Y}_{\text{bn}} &= \mathbf{S}(\mathbf{Y}_{\text{conv-int}} + \mathbf{B}_{\text{int}}) \\ \mathbf{Y}_{\text{relu-int}} &= \text{clip}(\text{round}(\mathbf{Y}_{\text{bn}}), \text{MIN}, \text{MAX}), \end{aligned} \quad (1)$$

where $\mathbf{Y}_{\text{conv-int}} \in \mathbb{Z}^{N \times H \times W \times C}$, $\mathbf{Y}_{\text{bn}} \in \mathbb{R}^{1 \times 1 \times 1 \times C}$ and $\mathbf{Y}_{\text{relu-int}} \in \mathbb{Z}^{N \times H \times W \times C}$ are the output of convolution, batch normalization, and activation function, respectively. $\mathbf{B}_{\text{int}} \in \mathbb{Z}^{1 \times 1 \times 1 \times C}$ is the bias. $\mathbf{S} = \frac{\mathbf{S}_{\mathbf{w}} \mathbf{S}_{\mathbf{x}}^i}{\mathbf{S}_{\mathbf{o}}^i} \in \mathbb{R}^{1 \times 1 \times 1 \times C}$, in which $\mathbf{S}_{\mathbf{w}} \in \mathbb{R}^{1 \times 1 \times 1 \times C}$

is the weight scaling factor, S_x^i is the scalar scaling factor for the input activation and S_x^o is the scalar re-quantization scaling factor for the output activation.

Looking back at our quantization, since ReLU executes maximum operation $\max(0, x)$ and the threshold \mathbf{Y}_{th} used in the quantization step is non-negative, the green part marked as *Forward Fusion* in Fig. 1 can be fused into the previous batch normalization layer. In addition, the nonlinearity function is no longer required. For the blue part marked as *Backward Fusion*, because of the linearity of convolution operation, its scalar scaling parameter, $\text{mean}(\mathbf{Y}_{\text{th}}^i)$, can be fused into the following batch-normalization layer. Eventually, for our quantization, Eq. (1) becomes

$$\begin{aligned} \mathbf{Y}_{\text{bn}} &= \mathbf{S}_{\text{th}}(\mathbf{Y}_{\text{conv_int}} + \mathbf{B}_{\text{int}}) \\ \mathbf{Y}_{\text{relu_int}} &= \text{clip}(\text{round}(\mathbf{Y}_{\text{bn}}), \mathbb{V}^-, \mathbb{V}^+), \end{aligned}$$

where $\mathbf{S}_{\text{th}} = \alpha \frac{S_w}{\mathbf{Y}_{\text{th}}^o} \in \mathbb{R}^{1 \times 1 \times 1 \times C}$, $\mathbf{Y}_{\text{th}}^o \in \mathbb{R}^{1 \times 1 \times 1 \times C}$ is the activation threshold of the output activation and $\alpha = \text{mean}(\mathbf{Y}_{\text{th}}^i)$ is a scalar value and equals to mean of the input activation threshold.

4. Experiments

In this section, we prove the feasibility of the double-stage-ST-based activation quantization and perform comparisons with previous works. We quantize both activation and weight with the same bit width. The weight quantization uses the method proposed by LSQ⁸. Same as previous work^{7-9,18}, the first and last layers keep full precision. All the experiments are done on dataset ImageNet²⁶.

4.1. Improvement of Double-Stage Squeeze-and-Threshold

In this subsection, we execute a comparison with previous work ST¹⁰ and show the improvement. To have a fair comparison, we use the same full precision model of ResNet18 as in ST, which is available on the PyTorch official website and can achieve a TOP1/TOP5 accuracy of 69.7%/89.1%. All of the training hyper-parameters are the same as ST, except the optimizer learning rate and weight decay. The comparison result is demonstrated in Table 1. As the result shows, compared to ST, our proposed double-stage ST improves the TOP1 accuracy of 1-bit, 2-bit, 3-bit, and 4-bit models by 0.2%, 0.4%,

1.0%, and 1.2%, respectively. Moreover, the accuracy of the 3-bit and 4-bit models of double-stage ST are beyond the full-precision accuracy. The detailed training settings are available in Appendix 1.

4.2. Comparison with state-of-the-art methods

In this subsection, we compare our double-stage ST method with state-of-the-art methods. The comparison result is available in Table 2. All the TOP1/TOP5 accuracy of other methods are from the original paper.

For the binary model, the comparison is executed on the ImageNet²⁶ dataset and ReActNet⁹ model. We use our double-stage-ST-based activation binarization to replace ReActNet’s original activation binarization. Same as the original work of ReActNet⁹, we train the network with two steps. Only activation is binarized in the first step, and weight is precisely trained. In the second step, the model is initialized with step one model. Then both activation and weight are binarized. The detailed training settings are available in Appendix B.

For the multi-bit models, the comparison is performed on the ImageNet²⁶ dataset and the ResNet-18²⁷ model. Since most state-of-the-art multi-bit quantization methods use a full-precision ResNet-18 with a TOP1/TOP5 accuracy of 70.5%/89.8%, for a fair comparison, we re-train ResNet-18 to achieve such accuracy and use it as the initial model for quantization. To achieve the best accuracy, we train the network with two steps as training ReActNet. The detailed training settings are in Appendix C.

5. Conclusion

In the actual application of ST quantification, we found that its input-channel-wise and output-channel-wise quantization weakened the efficiency of the quantization network and brought difficulties to deployment. As a result, we further investigate the attention mechanism and upgraded it to a two-stage ST. In the end, the two-stage ST quantization performs better than other competitors and demonstrates state-of-the-art results.

Acknowledgments

This work is funded by the German Re-

Table 1. Performance comparison between ST and double-stage ST. Comparison is evaluated by TOP1/TOP5 accuracy in percentage on ImageNet. The full-precision model ResNet-18 TOP1/TOP5 accuracy is 69.7%/89.1%.

Method	1-bit	2-bit	3-bit	4-bit
ST ¹⁰	57.5/80.4	66.7/86.9	68.8/88.5	69.5/88.9
Double-Stage ST (Ours)	57.9/80.6	67.1/87.3	69.8/89.1	70.7/89.6

Table 2. Performance comparison between double-stage ST and other state-of-art methods on ReActNet and ResNet-18. Comparison is evaluated by TOP1/TOP5 accuracy in percentage on ImageNet. ReActNet is trained from scratch and ResNet-18 quantization starts with a full-precision model with TOP1/TOP5 accuracy of 70.5%/89.8%.

Method	ResNet-18			ReActNet
	2-bit	3-bit	4-bit	1-bit
Double-Stage ST (Ours)	68.1/87.9	70.9/89.6	71.8/90.0	70.7/89.3
DDQ(2021) ²⁵	—/—	—/—	71.1/—	—/—
HAWQV3(2021) ²⁸	—/—	68.5/—	—/—	—/—
LSQ(2020) ⁸	67.9/88.1	70.6/89.7	71.2/90.1	—/—
DSQ(2019) ²⁹	65.2/—	68.7/—	69.6/—	—/—
LQ-Nets(2018) ³⁰	64.9/85.9	68.2/87.9	69.3/88.8	—/—
NICE(2018) ³¹	—/—	67.7/88.2	69.8/89.2	—/—
PACT(2018) ⁷	64.4/—	68.1/—	69.2/—	—/—
ReActNetAdam(2021) ³²	—/—	—/—	—/—	70.5/89.1
ReActNet(2020) ⁹	—/—	—/—	—/—	69.4/88.6

search Foundation (DFG, Deutsche Forschungsgemeinschaft) as part of Germany’s Excellence Strategy – EXC 2050/1 – Project ID 390696704 – Cluster of Excellence “Centre for Tactile Internet with Human-in-the-Loop” (CeTI) of Technische Universität Dresden.

We are grateful to the Centre for Information Services and High Performance Computing [Zentrum für Informationsdienste und Hochleistungsrechnen (ZIH)] TU Dresden for providing its facilities for high throughput calculations.

Appendix A Training setting for ResNet-18 binarization and quantization in Table 1

In this appendix, the training settings of models in Table 1 are listed in detail. The models were trained for 90 epochs with a batch size of 256 on two NVIDIA A100 GPUs. M_{min} is set to 0.1. The learning rate is set using a cosine annealing schedule with a minimum learning rate of 10^{-4} . Stochastic gradient descent (SGD) with momentum 0.9 and Nesterov

momentum is used for optimization. For the newly introduced operation, their trainable parameters are initialized with the default one in PyTorch. For the non-trainable parameter, the activation threshold is set to zero at the beginning. The weight quantization solution stays the same as ST.¹⁰ The optimizer initial learning rate γ for 1-bit, 2-bit, 3-bit, and 4-bit models are 0.125, 0.05, 0.035, and 0.025, respectively. Whereas the optimizer weight decay λ for 1-bit, 2-bit, 3-bit, and 4-bit models are 1×10^{-6} , 3×10^{-5} , 3×10^{-5} , and 3×10^{-5} , respectively. Whereas the optimizer weight decay λ is 1×10^{-6} for binarization and 3×10^{-5} for multi-bit quantization.

Appendix B Training setting for ReActNet in Table 2

For the newly introduced hyperparameter M_{min} , we set $M_{min} = 0.1$. ResNet-101 is used as the teacher model. All of the training hyper-parameters are the same as original ReActNet³², except the optimizer learning rate and weight decay shown in Ta-

ble C.2. The initial learning rate γ and weight decay λ are 0.75×10^{-3} and 1×10^{-6} in the first step, and 0.5×10^{-3} and 0.0 in the next step.

Appendix C Training setting for ResNet-18 binarization and quantization in Table 2

In this appendix, the training settings of models in Table 2 are listed in detail. For the ResNet-18 quantized model, we employ two-step training. In the first step, the model is initialized with the full-precision model with TOP1/TOP5 accuracy of 70.5%/89.8% and only activation is quantized. In the second step, the model is initialized with the model from step one. Both activation and weight are quantized. Furthermore, we apply labeling smoothing³³ with a factor of 0.1. Table C.1 shows the SGD optimizer’s initial learning rate γ and weight decay λ . The other training settings are the same as in Appendix 1.

Table C.1. Initial learning rate γ and weight decay λ settings for ResNet-18 quantization. The precision "AxWy" represents x -bit activation and y -bit weight.

Model	step	precision	γ	λ
2-bit	step1	A2W32	0.1	4×10^{-6}
	step2	A2W2	0.05	4×10^{-6}
3-bit	step1	A3W32	0.035	7×10^{-6}
	step2	A3W3	0.035	7×10^{-6}
4-bit	step1	A4W32	0.025	1×10^{-5}
	step2	A4W4	0.025	1×10^{-5}

The achieved TOP1/TOP5 accuracy of each step of the ResNet-18 quantized models are shown in Table C.2

Table C.2. TOP1/TOP5 accuracy of each step of the ResNet-18 quantized models. The corresponding full-precision ResNet-18 has a TOP1/TOP5 accuracy of 70.5/89.8.

model	step	precision	TOP1/TOP5
2-bit	step1	A2W32	69.162/88.386
	step2	A2W2	68.114/87.884
3-bit	step1	A3W32	71.342/89.848
	step2	A3W3	70.906/89.560
4-bit	step1	A4W32	71.804/90.192
	step2	A4W4	71.822/89.988

Bibliography

1. B. Jacob, S. Kligys, B. Chen, M. Zhu, M. Tang, A. G. Howard, H. Adam and D. Kalenichenko, Quantization and training of neural networks for efficient integer-arithmetic-only inference, *2018 IEEE Conference on Computer Vision and Pattern Recognition, CVPR 2018, Salt Lake City, UT, USA, June 18-22, 2018*, (IEEE Computer Society, 2018), pp. 2704–2713.
2. Y. L. Cun, J. S. Denker and S. A. Solla, *Optimal Brain Damage, Advances in Neural Information Processing Systems 2* (Morgan Kaufmann Publishers Inc., San Francisco, CA, USA, 1990), San Francisco, CA, USA, p. 598–605.
3. S. Han, J. Pool, J. Tran and W. J. Dally, Learning both weights and connections for efficient neural networks, *Proceedings of the 28th International Conference on Neural Information Processing Systems - Volume 1, NIPS’15*, (MIT Press, Cambridge, MA, USA, 2015), p. 1135–1143.
4. A. Howard, R. Pang, H. Adam, Q. V. Le, M. Sandler, B. Chen, W. Wang, L. Chen, M. Tan, G. Chu, V. Vasudevan and Y. Zhu, Searching for mobilenetv3, *2019 IEEE/CVF International Conference on Computer Vision, ICCV 2019, Seoul, Korea (South), October 27 - November 2, 2019*, (Computer Vision Foundation / IEEE Computer Society, 2019), pp. 1314–1324.
5. M. Abadi, P. Barham, J. Chen, Z. Chen, A. Davis, J. Dean, M. Devin, S. Ghemawat, G. Irving, M. Isard, M. Kudlur, J. Levenberg, R. Monga, S. Moore, D. G. Murray, B. Steiner, P. Tucker, V. Vasudevan, P. Warden, M. Wicke, Y. Yu and X. Zheng, Tensorflow: A system for large-scale machine learning, *Proceedings of the 12th USENIX Conference on Operating Systems Design and Implementation, OSDI’16*, (USENIX Association, USA, 2016), p. 265–283.
6. A. Paszke, S. Gross, F. Massa, A. Lerer, J. Bradbury, G. Chanan, T. Killeen, Z. Lin, N. Gimelshein, L. Antiga, A. Desmaison, A. Köpf, E. Yang, Z. DeVito, M. Raison, A. Tejani, S. Chilamkurthy, B. Steiner, L. Fang, J. Bai and S. Chintala, Pytorch: An imperative style, high-performance deep learning library, *Advances in Neural Information Processing Systems 32: Annual Conference on Neural Informa-*

- tion Processing Systems 2019, NeurIPS 2019, 8-14 December 2019, Vancouver, BC, Canada, eds. H. M. Wallach, H. Larochelle, A. Beygelzimer, F. d'Alché-Buc, E. B. Fox and R. Garnett (MIT Press, 2019), pp. 8024–8035.
7. J. Choi, Z. Wang, S. Venkataramani, P. I. Chuang, V. Srinivasan and K. Gopalakrishnan, PACT: parameterized clipping activation for quantized neural networks, *CoRR* **abs/1805.06085** (2018).
 8. S. K. Esser, J. L. McKinstry, D. Bablani, R. Appuswamy and D. S. Modha, Learned step size quantization, *8th International Conference on Learning Representations, ICLR 2020, Addis Ababa, Ethiopia, April 26-30, 2020*, (OpenReview.net, 2020).
 9. Z. Liu, Z. Shen, M. Savvides and K.-T. Cheng, Re-actnet: Towards precise binary neural network with generalized activation functions, *Computer Vision – ECCV 2020*, eds. A. Vedaldi, H. Bischof, T. Brox and J.-M. Frahm (Springer International Publishing, Cham, 2020), pp. 143–159.
 10. B. Wu, B. Waschneck and C. Mayr, Squeeze-and-threshold based quantization for low-precision neural networks, *Proceedings of the 22nd Engineering Applications of Neural Networks Conference*, eds. L. Iliadis, J. Macintyre, C. Jayne and E. Pimenidis (Springer International Publishing, Cham, 2021), pp. 232–243.
 11. K. Hwang and W. Sung, Fixed-point feedforward deep neural network design using weights +1, 0, and -1, *2014 IEEE Workshop on Signal Processing Systems (SiPS)*, (IEEE, 2014), pp. 1–6.
 12. I. Hubara, M. Courbariaux, D. Soudry, R. El-Yaniv and Y. Bengio, Binarized neural networks, *Advances in Neural Information Processing Systems 29: Annual Conference on Neural Information Processing Systems 2016, December 5-10, 2016, Barcelona, Spain*, eds. D. D. Lee, M. Sugiyama, U. von Luxburg, I. Guyon and R. Garnett (MIT Press, 2016), pp. 4107–4115.
 13. G. Hinton, L. Deng, D. Yu, G. E. Dahl, A. rahman Mohamed, N. Jaitly, A. Senior, V. Vanhoucke, P. Nguyen, T. N. Sainath and B. Kingsbury, Deep neural networks for acoustic modeling in speech recognition: The shared views of four research groups, *IEEE Signal Processing Magazine* **29**(6) (2012) 82–97.
 14. S. Darabi, M. Belbahri, M. Courbariaux and V. P. Nia, BNN+: improved binary network training, *CoRR* **abs/1812.11800** (2018).
 15. M. Rastegari, V. Ordonez, J. Redmon and A. Farhadi, Xnor-net: Imagenet classification using binary convolutional neural networks, *Computer Vision - ECCV 2016 - 14th European Conference, Amsterdam, The Netherlands, October 11-14, 2016, Proceedings, Part IV*, eds. B. Leibe, J. Matas, N. Sebe and M. Welling *Lecture Notes in Computer Science* **9908**, (Springer, 2016), pp. 525–542.
 16. A. Bulat and G. Tzimiropoulos, Xnor-net++: Improved binary neural networks, *30th British Machine Vision Conference 2019, BMVC 2019, Cardiff, UK, September 9-12, 2019*, (BMVA Press, 2019), p. 62.
 17. Z. Liu, B. Wu, W. Luo, X. Yand, W. Liu and K.-T. Cheng, Bi-real net: Binarizing deep network towards real-network performance, *International Journal of Computer Vision (IJCV)* **128**(1) (2020) 202–219.
 18. J. Bethge, H. Yang, M. Bornstein and C. Meinel, Binarydensenet: Developing an architecture for binary neural networks, *2019 IEEE/CVF International Conference on Computer Vision Workshops, ICCV Workshops 2019, Seoul, Korea (South), October 27-28, 2019*, (IEEE, 2019), pp. 1951–1960.
 19. J. Bethge, C. Bartz, H. Yang, Y. Chen and C. Meinel, Meliusnet: An improved network architecture for binary neural networks, *IEEE Winter Conference on Applications of Computer Vision, WACV 2021, Waikoloa, HI, USA, January 3-8, 2021*, (IEEE, 2021), pp. 1438–1447.
 20. H. Qin, R. Gong, X. Liu, M. Shen, Z. Wei, F. Yu and J. Song, Forward and backward information retention for accurate binary neural networks, *2020 IEEE/CVF Conference on Computer Vision and Pattern Recognition, CVPR 2020, Seattle, WA, USA, June 13-19, 2020*, (IEEE, 2020), pp. 2247–2256.
 21. S. Zhou, Z. Ni, X. Zhou, H. Wen, Y. Wu and Y. Zou, Dorefa-net: Training low bitwidth convolutional neural networks with low bitwidth gradients, *CoRR* **abs/1606.06160** (2016).
 22. Z. Cai, X. He, J. Sun and N. Vasconcelos, Deep learning with low precision by half-wave gaussian quantization, *2017 IEEE Conference on Computer Vision and Pattern Recognition, CVPR 2017, Honolulu, HI, USA, July 21-26, 2017*, (IEEE, 2017), pp. 5406–5414.
 23. B. Zhuang, L. Liu, M. Tan, C. Shen and I. Reid, Training quantized neural networks with a full-precision auxiliary module, *2020 IEEE/CVF Conference on Computer Vision and Pattern Recognition (CVPR)*, (IEEE, 2020), pp. 1485–1494.
 24. C. Louizos, M. Reisser, T. Blankevoort, E. Gavves and M. Welling, Relaxed quantization for discretized neural networks, *7th International Conference on Learning Representations, ICLR 2019, New Orleans, LA, USA, May 6-9, 2019*, (OpenReview.net, 2019).
 25. Z. Zhang, W. Shao, J. Gu, X. Wang and P. Luo, Differentiable dynamic quantization with mixed precision and adaptive resolution, *Proceedings of the 38th International Conference on Machine Learning, ICML 2021, 18-24 July 2021, Virtual Event*, (OpenReview.net, 2021), pp. 12546–12556.
 26. J. Deng, W. Dong, R. Socher, L.-J. Li, K. Li and L. Fei-Fei, Imagenet: A large-scale hierarchical image database, *2009 IEEE Conference on Computer Vision and Pattern Recognition*, (IEEE, 2009), pp. 248–255.
 27. K. He, X. Zhang, S. Ren and J. Sun, Deep resid-

- ual learning for image recognition, *2016 IEEE Conference on Computer Vision and Pattern Recognition, CVPR 2016, Las Vegas, NV, USA, June 27-30, 2016*, (IEEE Computer Society, 2016), pp. 770–778.
28. Z. Yao, Z. Dong, Z. Zheng, A. Gholami, J. Yu, E. Tan, L. Wang, Q. Huang, Y. Wang, M. W. Mahoney and K. Keutzer, HAWQV3: dyadic neural network quantization, *CoRR* **abs/2011.10680** (2020).
 29. R. Gong, X. Liu, S. Jiang, T. Li, P. Hu, J. Lin, F. Yu and J. Yan, Differentiable soft quantization: Bridging full-precision and low-bit neural networks, *2019 IEEE/CVF International Conference on Computer Vision, ICCV 2019, Seoul, Korea (South), October 27 - November 2, 2019*, (IEEE, 2019), pp. 4851–4860.
 30. D. Zhang, J. Yang, D. Ye and G. Hua, Lq-nets: Learned quantization for highly accurate and compact deep neural networks, *Computer Vision – ECCV 2018*, eds. V. Ferrari, M. Hebert, C. Sminchisescu and Y. Weiss (Springer International Publishing, Cham, 2018), pp. 373–390.
 31. C. Baskin, N. Liss, Y. Chai, E. Zheltonozhskii, E. Schwartz, R. Giryes, A. Mendelson and A. M. Bronstein, NICE: noise injection and clamping estimation for neural network quantization, *CoRR* **abs/1810.00162** (2018).
 32. Z. Liu, Z. Shen, S. Li, K. Helwegen, D. Huang and K. Cheng, How do adam and training strategies help bnns optimization?, *CoRR* **abs/2106.11309** (2021).
 33. C. Szegedy, V. Vanhoucke, S. Ioffe, J. Shlens and Z. Wojna, Rethinking the inception architecture for computer vision, *2016 IEEE Conference on Computer Vision and Pattern Recognition (CVPR)*, (IEEE Computer Society, Los Alamitos, CA, USA, jun 2016), pp. 2818–2826.